

Electronic Supporting Information (ESI) for:

Silicon photosensitisation using molecular layers

Lefteris Danos^{1}, Nathan R. Halcovitch¹, Ben Wood¹, Henry Banks¹, Michael P. Coogan¹,
Nicholas Alderman², Liping Fang³, Branislav Dzurnak⁴, and Tom Markvart^{4,5}*

¹Department of Chemistry, Energy Lancaster, Lancaster University, Lancaster, LA1 4YB, UK

²Department of Chemistry, University of Ottawa, Ottawa K1N 6N5, Canada

³Department of Electrical and Electronic Engineering, Southern University of Science and
Technology, Shenzhen, Guangdong, China 518055

⁴Centre for Advanced Photovoltaics, Czech Technical University, 166 27 Prague, Czech Republic

⁵Solar Energy Laboratory, Faculty of Engineering and the Environment, University of Southampton,
Southampton, SO17 1BJ, UK

Experimental Details

Synthesis of Dibromo benzoic perylene diimide (Di-Br-Pe)

Elemental analysis was used to check the purity (Elementar MicroCube S/N: 15143037): Calculated (%) C: 61.74; H: 2.30; N: 4.00; Found (%) C: 62.36; H: 2.41; N: 4.48.

Synthesis of Bis(n-decylimido)perylene (PTCD-C10)

Recrystallisation from chloroform by addition of methanol gave: C 76.28 H 6.90 N 3.86 %, $C_{44}H_{50}N_2O_4 \cdot 0.2CHCl_3$ requires C 76.4 H 7.29 N 4.03%. ¹H NMR (CDCl₃, 400 MHz) δ H 8.73 (4H, d, J = 8.1 Hz, ArH-2,5,8,11) 8.66 (4H, d, J = 8.1 Hz, ArH-1,6,7,12) 4.23 (4H, t, J = 7.5 Hz, 2 x N-CH₂) 1.8-1.2 (m, 2x (CH₂)₈)* 0.89 (m, 6H, 2 x Me).

NMR spectra were recorded on a Bruker Avance 400 MHz spectrometer at 400 MHz (¹H) or 100 MHz (¹³C) at 25 °C in 5 mm NMR tubes.

*due to low solubility insufficient signal to noise was obtained to allow resolution and accurate integration of the aliphatic chain or ¹³C data.

Time resolved emission spectra and fluorescence decays

The fluorescence decay intensities were analysed using a multi-exponential model (Reconvolution) as the sum of single exponential decay curves:¹

$$I(t) = \sum_{i=1}^n A_i \cdot e^{-\frac{t}{\tau_i}} \quad (\text{Eq. S1})$$

where τ_i are the decay lifetimes with amplitudes A_i of the components at $t = 0$ and n is the number of decay lifetimes.

The fractional contribution (f_i) of each decay component to the steady state intensity is given by

$$f_i = \frac{A_i \cdot \tau_i}{\sum_j A_j \cdot \tau_j} \quad (\text{Eq. S2})$$

The average lifetimes can be defined in two ways and they differ in the way the decay lifetimes are weighted in the averaging

$$\tau_{AV1} = \frac{\sum_i A_i \cdot \tau_i^2}{\sum_i A_i \cdot \tau_i} \quad (\text{Eq. S3})$$

τ_{AV1} equals the average amount of time the fluorophore remains in the excited state after the start of the excitation

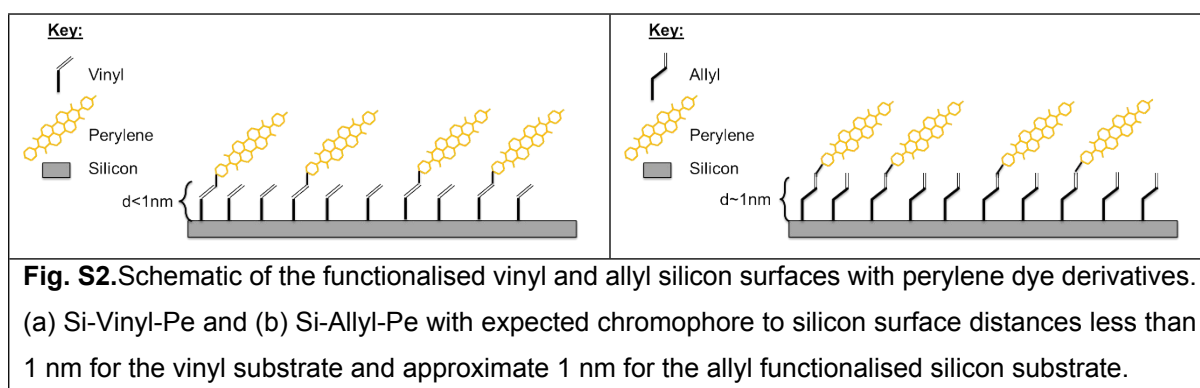
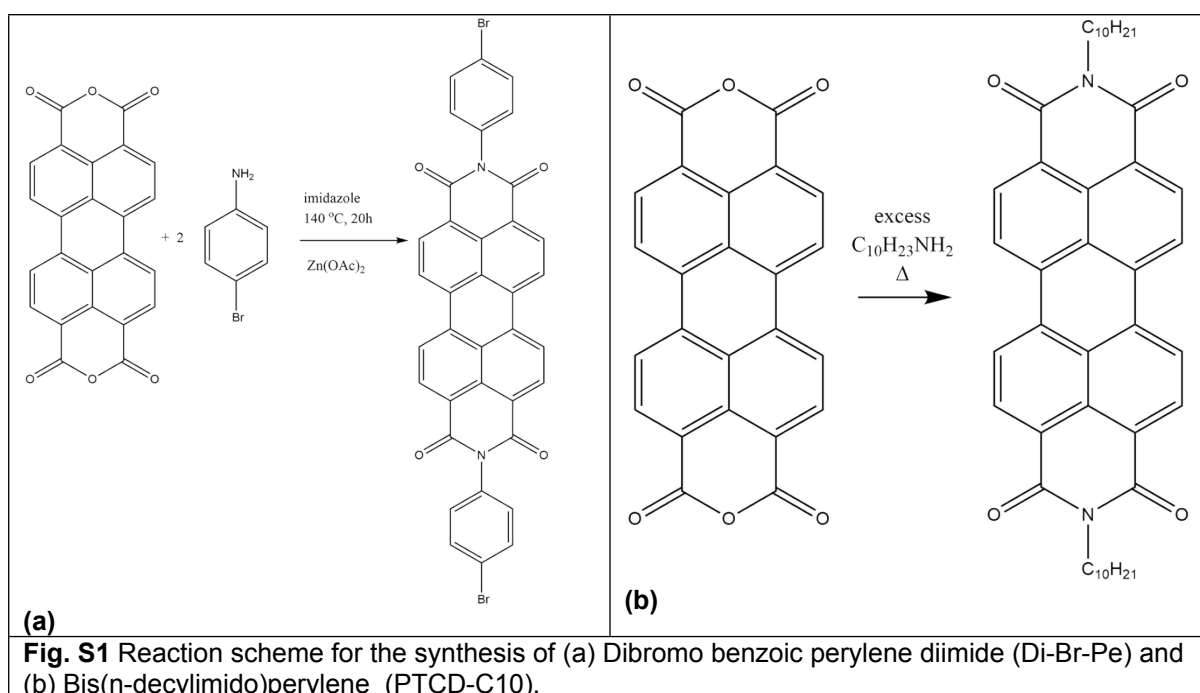
$$\tau_{AV2} = \frac{\sum_i A_i \cdot \tau_i}{\sum_i A_i} \quad (\text{Eq. S4})$$

τ_{AV2} is proportional to the area under the decay curve and is mainly used in lifetime based energy transfer efficiency estimation.

$$E = 1 - \frac{F_{DA}}{F_D} = 1 - \frac{\int I_{DA}(t) dt}{\int I_D(t) dt} \quad (\text{Eq. S5})$$

where $I_{DA}(t)$ and $I_D(t)$ are the intensity decays of the donor in the presence and absence of the acceptor energy transfer respectively. The integrals are proportional to the steady state fluorescence intensities in the presence (F_{DA}) and absence (F_D) of the acceptor energy transfer.

List of Figures



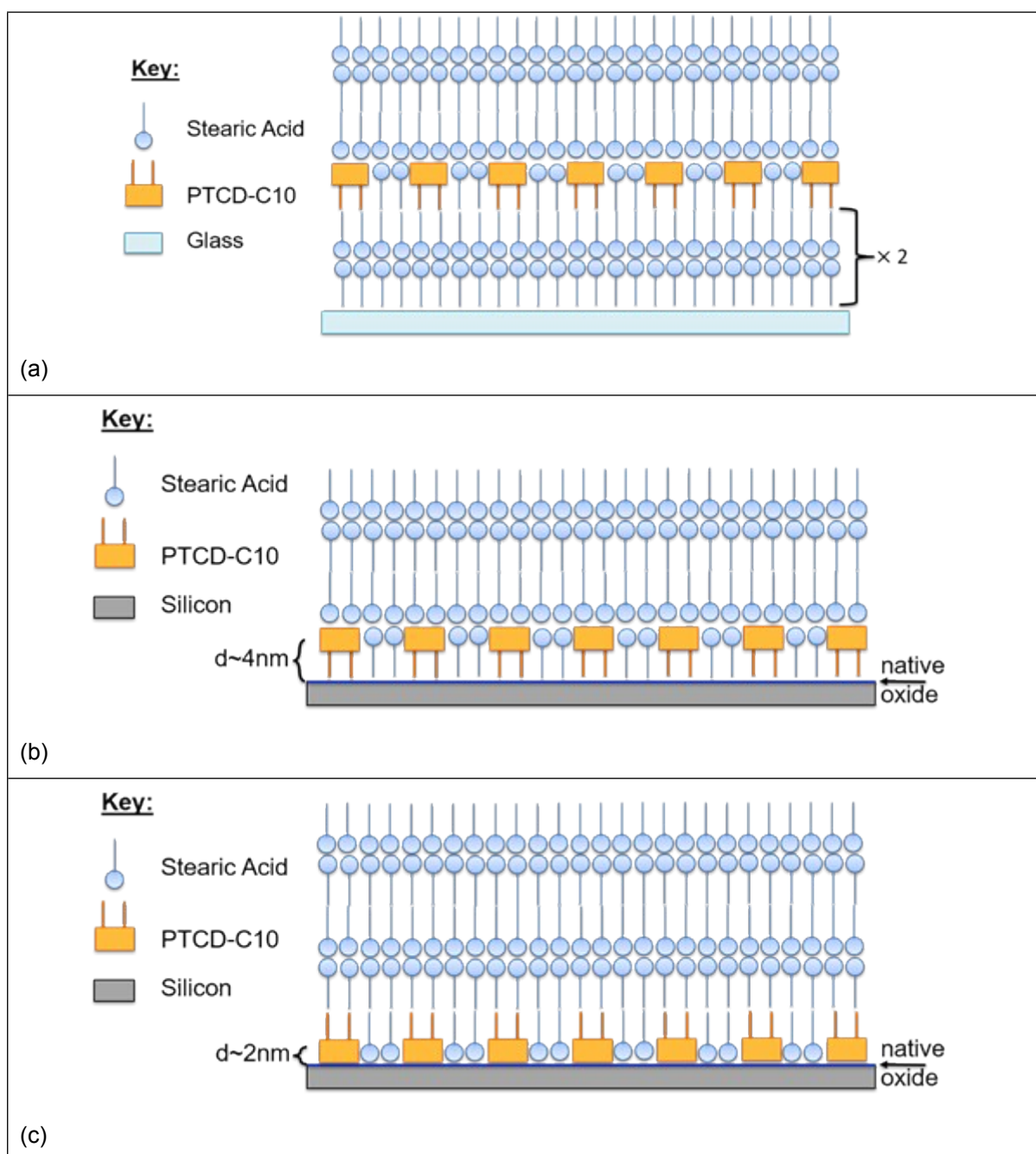
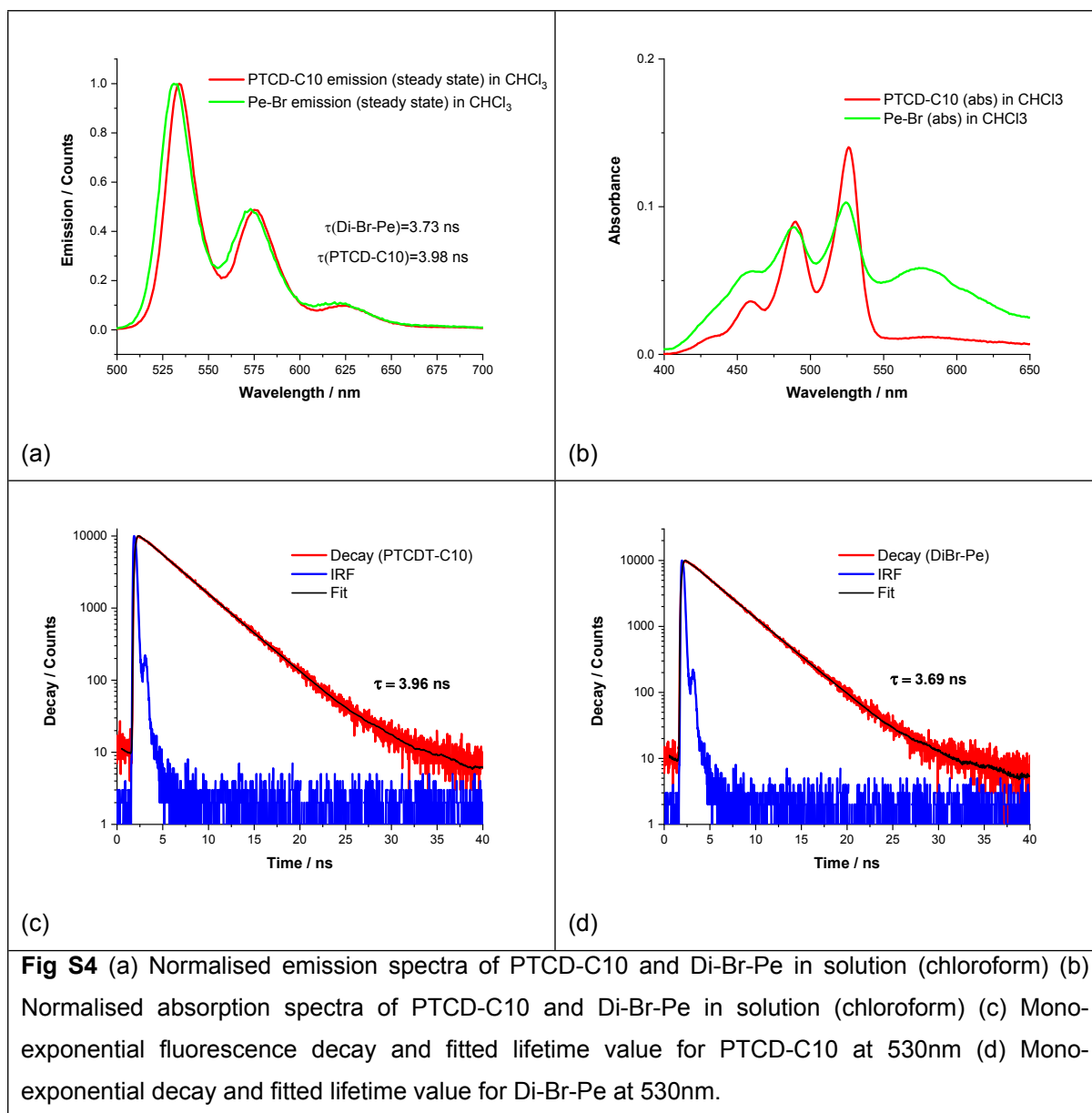


Fig S3 (a) Schematic of PTCD-C10 mixed dye monolayer deposited on a glass substrate. Four monolayers of stearic acid (SA) were first deposited followed by a monolayer of PTCD-C10 at a mixing ratio of 1:25 with SA. The monolayer was capped with 3 layers of SA. (b) & (c) two different orientations of the PTCD-10 monolayer deposited on a hydrophobic (**LB2**) treated and hydrophilic (**LB1**) treated silicon surface. The monolayer was capped with 3 layers of SA. The approximate distance of the chromophore to the silicon surface is indicated in the presence of the native oxide.



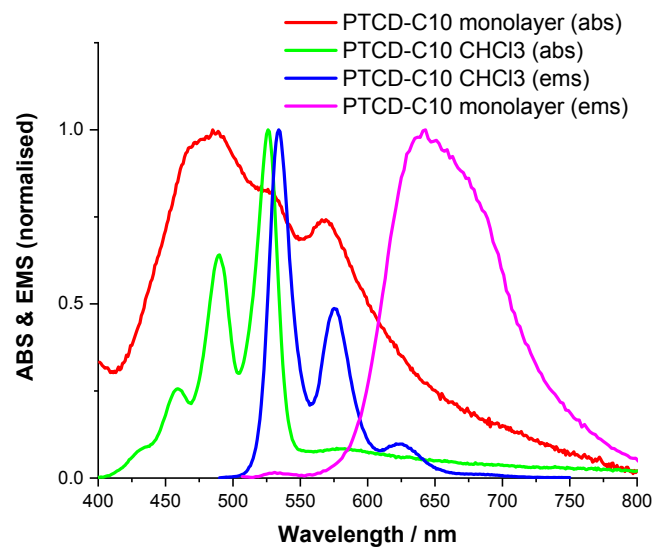
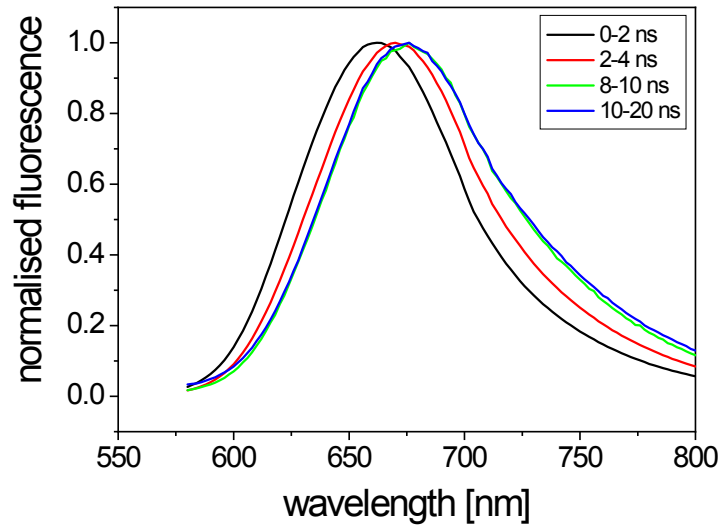
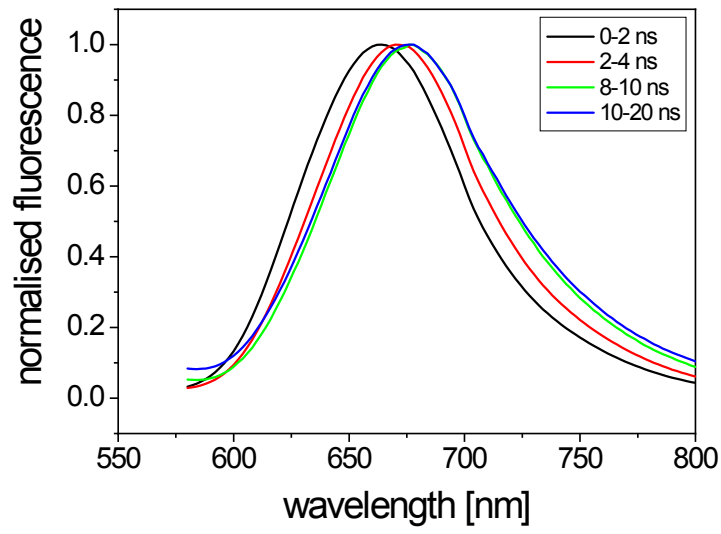


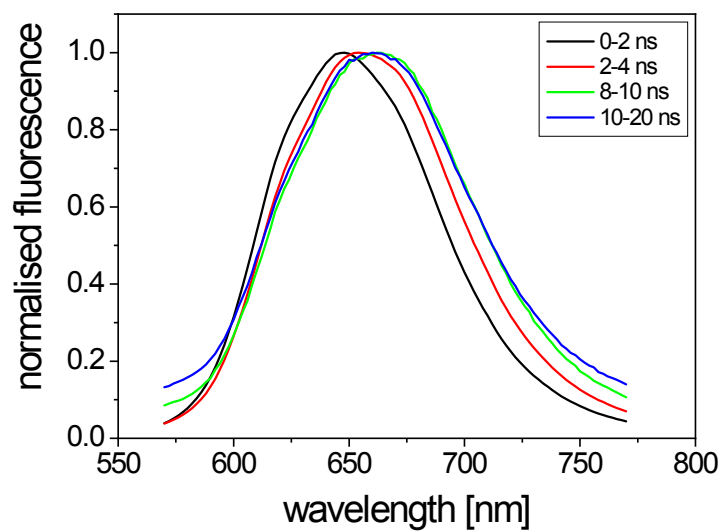
Fig. S5 (a) Normalised absorption and emission spectra of PTC-D-C10 dissolved in chloroform and deposited on glass as a mixed LB monolayer (PTCD-C10:SA) with SA in a 1:25 molar ratio



(a)

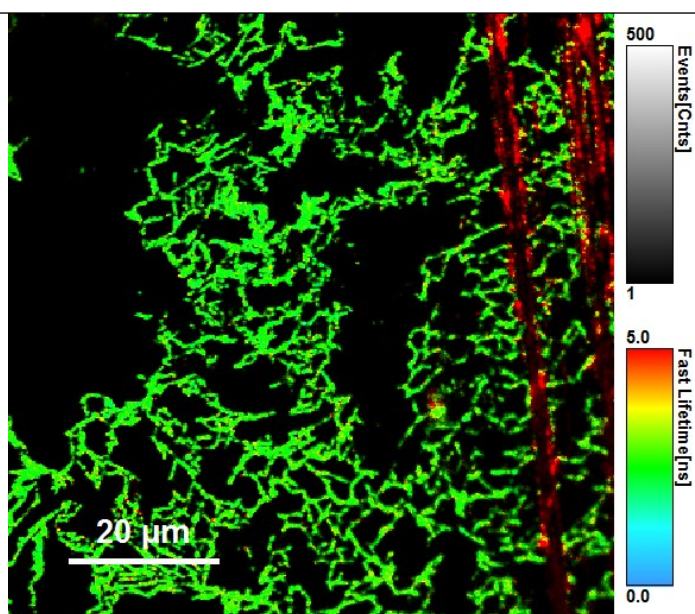


(b)

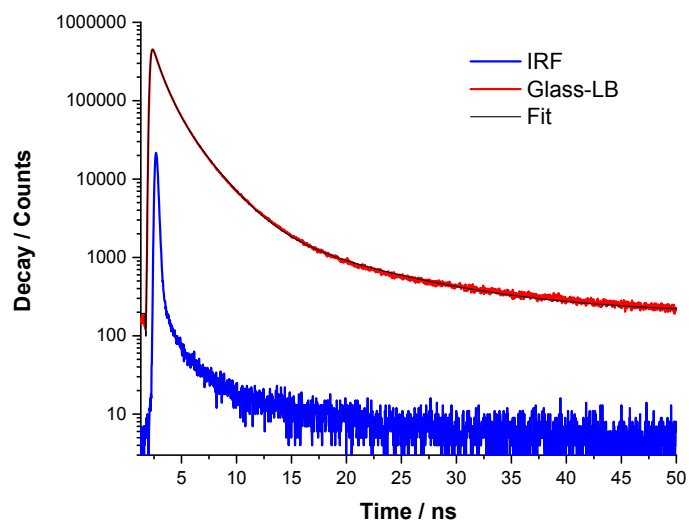


(c)

Fig. S6 TRES spectra for different mixing ratios of PTCD-C10 monolayers deposited on glass. The spectra are integrated over different times for (a) PTCD-C10:SA (1:1), (b) PTCD-C10:SA 1:10, (c) PTCD-C10:SA (1:25)

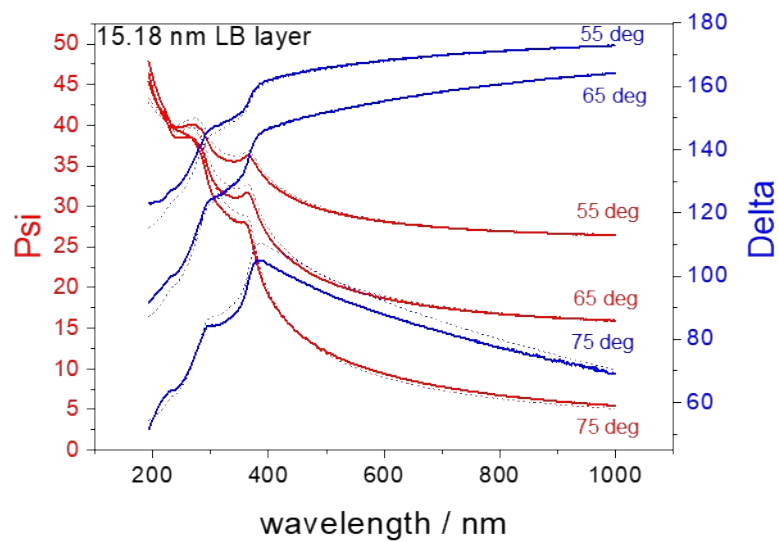


(a)

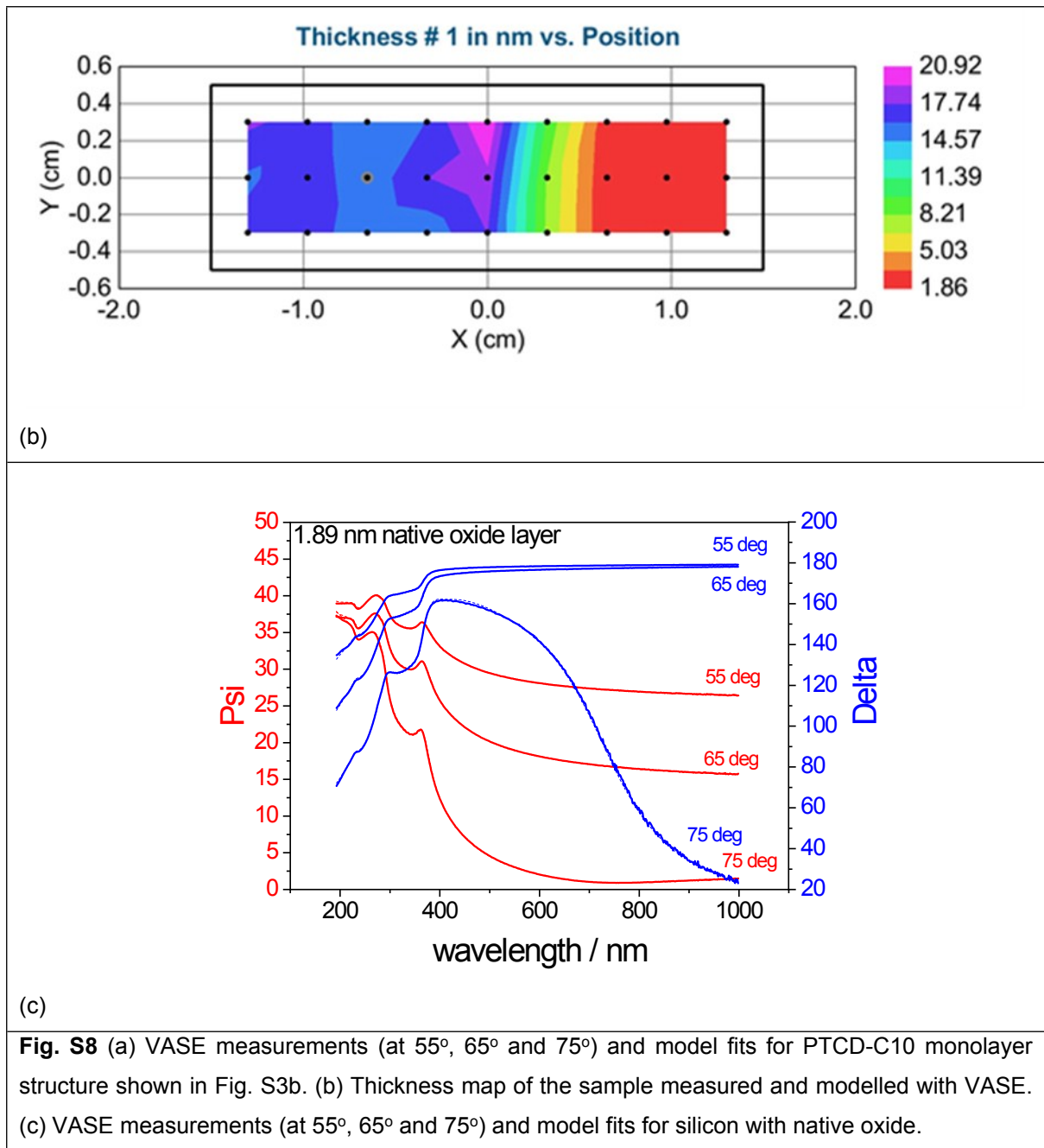


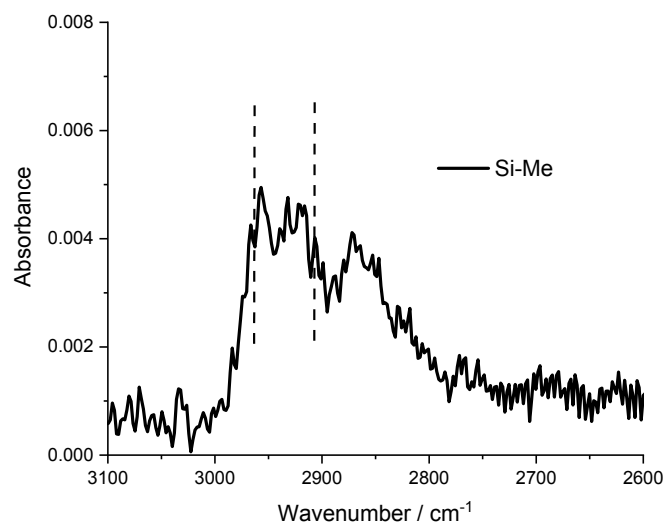
(b)

Fig. S7 (a) FLIM image of mixed monolayer (PTCD-C10:SA) deposited on glass with SA in a 1:25 molar ratio. (b) Overall decay and fit for FLIM image. The IRF is shown.

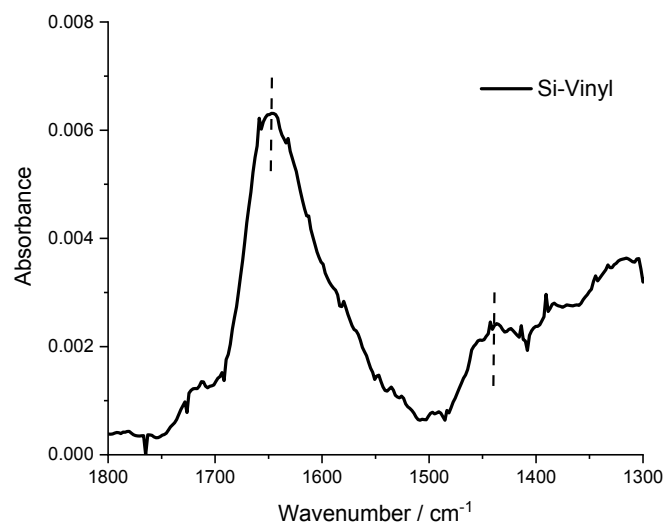


(a)

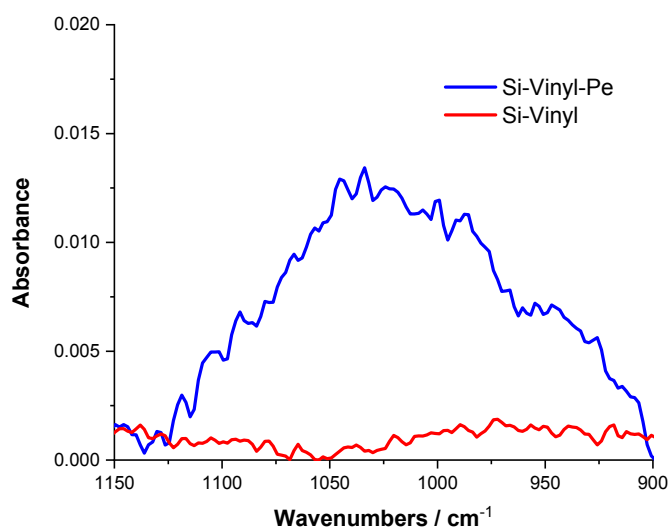




(a)

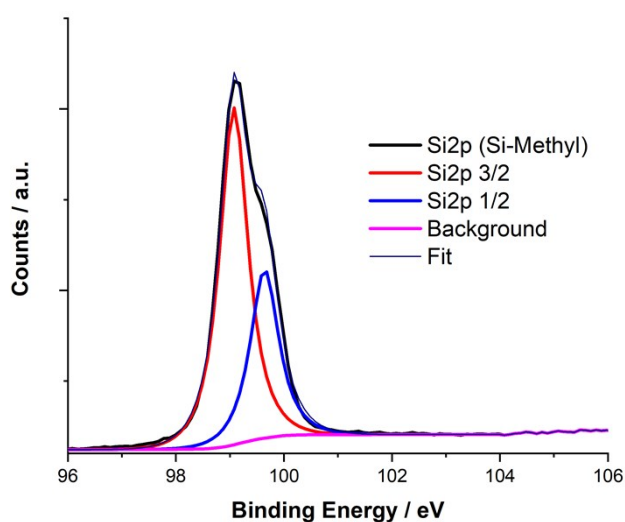


(b)

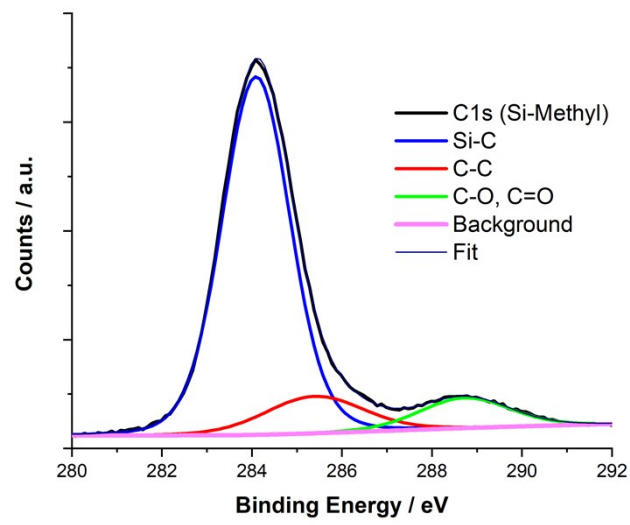


(c)

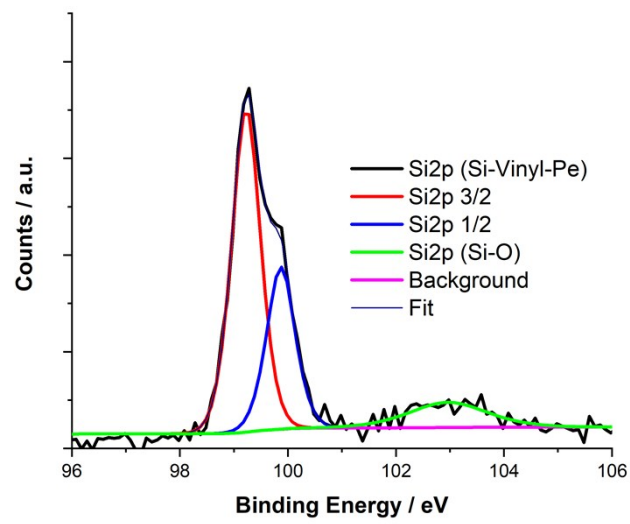
Fig. S9 (a) Transmission IR spectra of the C-H stretching region for Si(111)-Me surface. Peaks at 2909 cm⁻¹ and 2965 cm⁻¹ are indicated on the spectra and correspond to the C-H symmetric and asymmetric stretching modes respectively.^{2,3} Peaks at 2856 cm⁻¹ and 2928 cm⁻¹ arise from adventitious hydrocarbon adsorbed on the surface (from the solvents used in the synthesis)
 (b) Polarised reflection IR spectra showing the C=C stretch peak and C=C-H out of plane bend peak for a Si(111)-Vinyl surface. (c) Polarised reflection IR spectra showing the C-N stretching vibration region for Si(111)-Vinyl-Pe sample in comparison with Si(111)-Vinyl.



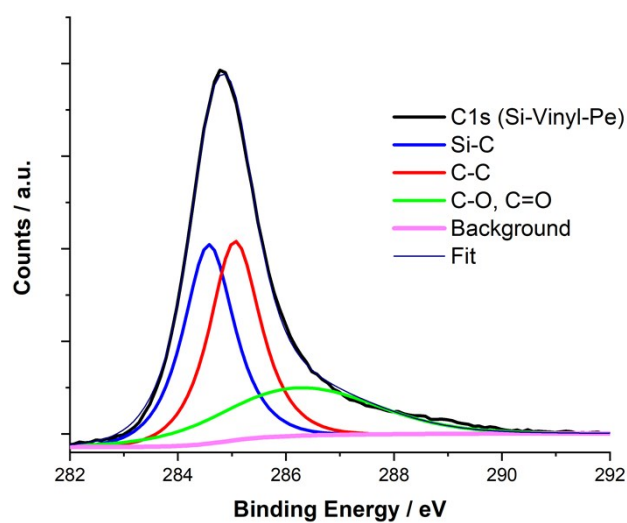
(a)



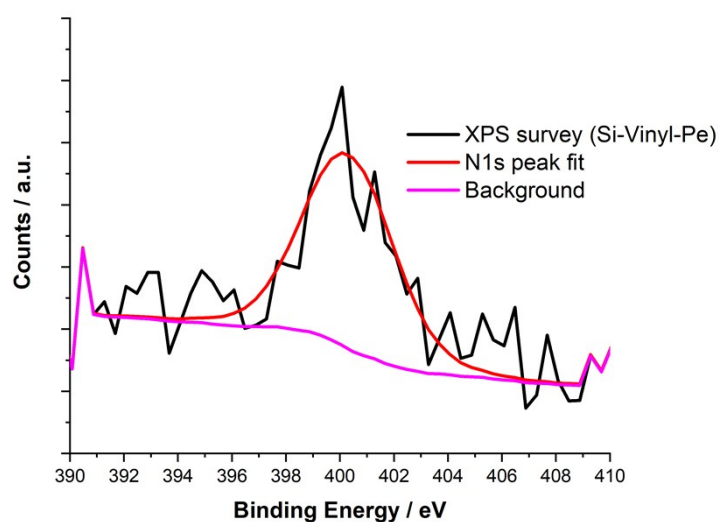
(b)



(c)

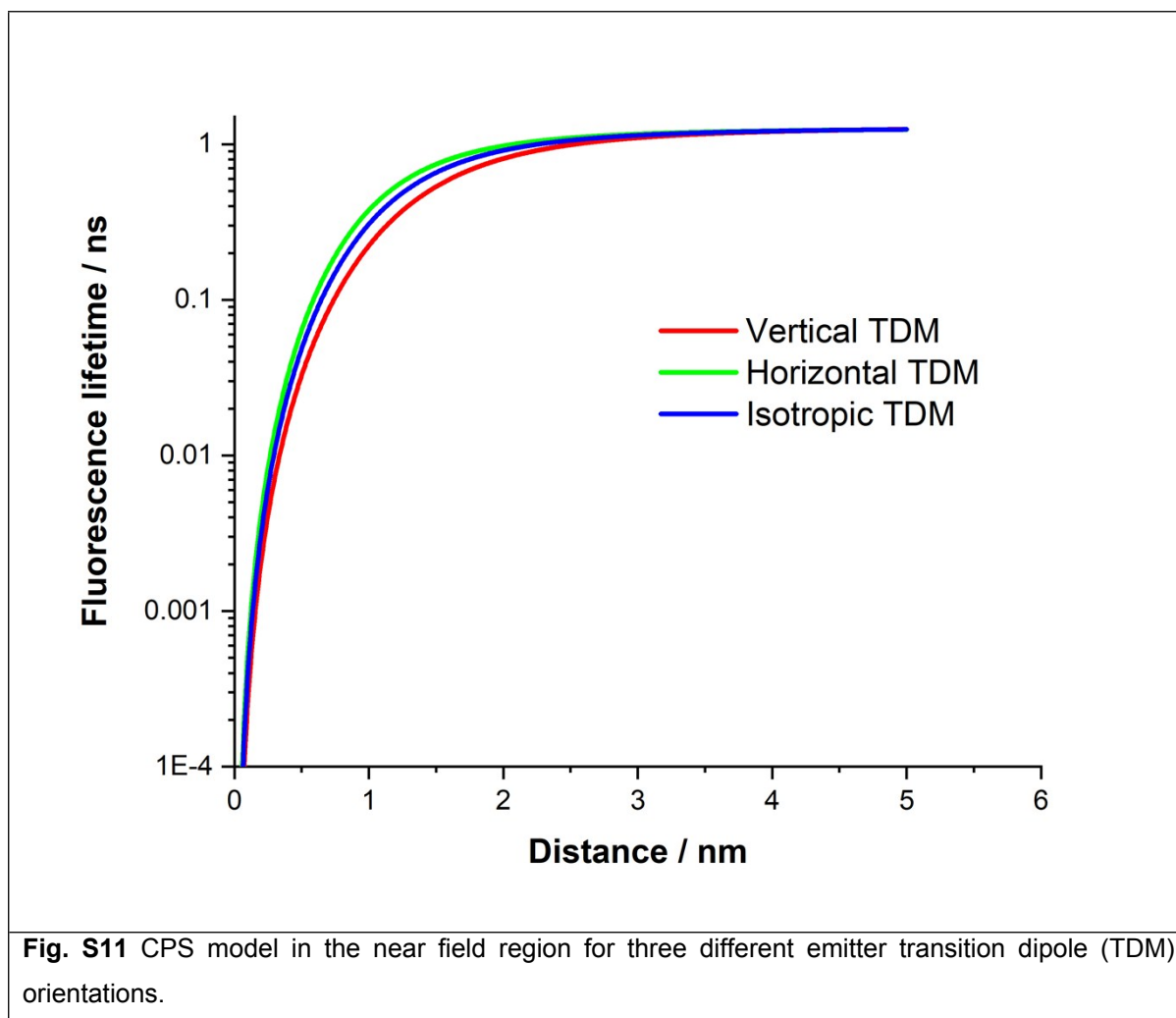


(d)



(e)

Fig. S10 (a) High resolution XPS spectra of the Si2p region for the Si(111)-Me surface showing Si2p 3/2 (red) and Si2p 1/2 (blue). (b) High resolution XPS spectra of the C1s region for the Methyl terminated Si (111) surface showing C-Si (blue), C-C (red), and C-O (green). (c) High resolution XPS spectra of the Si2p region for the Si(111)-Vinyl-Pe surface showing Si2p 3/2 (red) and Si2p 1/2 (blue) and Si-O (green). (d) High resolution XPS spectra of the C1s region for the Si(111)-Vinyl –Pe surface showing C-Si (blue), C-C or C-H (red), and C-O and C=O (green) (e) XPS spectra of the N1s region for the Si(111)-Vinyl–Pe surface.



References

- 1 K. Ray, R. Badugu and J. R. Lakowicz, *Langmuir*, 2006, **22**, 8374–8378.
- 2 L. J. Webb, S. Rivillon, D. J. Michalak, Y. J. Chabal and N. S. Lewis, *J. Phys. Chem. B*, 2006, **110**, 7349–7356.
- 3 N. Alderman, L. Danos, M. C. Grossel and T. Markvart, *RSC Adv.*, 2012, **2**, 7669–7672.